한국해양공학회 2006년도 추계학술대회 국제워크샵 pp.135~140

Numerical Computations of Extreme Wave Load on a Cylinder Using Frequency-Focusing Unidirectional Waves

JO-HYUN KYOUNG, SA-YOUNG HONG AND HONG-GUN SUNG

Offshore Plant Research Division, MOERI/KORDI, Daejon, Korea

KEY WORDS: Extreme Waves, Frequency Focusing, Wave Loads, Potential Flow, Finite Element Method

ABSTRACT: *Numerical computations are made to predict wave loads on a vertical cylinder in an extreme wave. To generate the extreme wave, a frequency-focused unidirectional wave is adopted in three-dimensional numerical wave tank. The mathematical formulation is made in the scope of the potential theory with fully nonlinear free surface conditions. As a numerical method, finite element method based on variational principle is applied. Comparisons between the present numerical results and the previous computation data show a good agreement.*

1. Introduction

The wave load and its influence on the response of offshore structure have been well investigated through the statistical approach based on the linear theory. Linear approach is applicable to estimate the operability of offshore structure in operational condition. But this approach has a limitation to apply the extreme condition such as freak wave, which corresponds to extreme value of wave spectrum.

The extreme wave such as freak wave has a wave height twice times larger than ordinary significant wave height. Peregrine(1976) has reported that this extreme wave can occur where the water depth is relatively shallow or there is an interaction between wave and current. This extreme wave can be occurred by the superposition of waves that have similar frequencies. The experiments by Chaplin et al.(1997) has shown that the extreme wave can be made by frequency focusing.

The extreme wave can be occurred in deep sea. In this case its wave height is around 30m. The extreme wave is easy to be a breaking wave and produces extreme wave load about 100 ton/m^2. Generally the design load of an ocean going vessel is about 15ton/m^2. Therefore the extreme wave can be expected to make abnormally severe damages on offshore structure.

경조현: 대전광역시 유성구 장동 171

042-868-7522 johyun@moeri.re.kr

In addition, the wave slope of extreme wave is quite large so that the ocean-going vessel could be capsized.

So investigation on characteristics of extreme wave as well as the generation mechanism is very important to safety, survivability and operability of offshore structures. There are two kind of well-known method for the generation of extreme wave. One is to use the frequency-focusing unidirectional wave. There have been many numerical and experimental studies using the frequency focusing(Hong et al., 2002; Zou & Kim, 1995; Chaplin, 1996; Clauss, 1999; Smith & Swan, 2002; Contento et al., 2001, Kim et al., 2004). The other is based on the self-modulation of wave induced by nonlinear wave-wave interaction. Stokes wave instability is well known for inducing such a self modulation(McClean, 1982). Weakly nonlinear wave model such as cubic nonlinear Schrödinger equation has been applied to explain the nonlinear wave-wave interaction related to the generation of extreme wave(Trulsen & Dysthe, 1997; Osborne, 2001; Grue, 2002).

The main topic of present study is to develop an efficient numerical method to predict wave load induced by extreme wave. The frequency-focusing method is applied. The wave load on the bottom mounted vertical cylinder is investigated. As a numerical method, finite element method based on variational principled is adopted. The nonlinear free surface problem is solved in time domain by utilizing potential flow. The wave elevation and wave load are obtained and compared with previous research.

2. Mathematical Formulation

To describe the nonlinear free surface motion efficiently, the Cartesian coordinate is adopted as the coordinate system. The positive z axis is taken opposite to the direction of gravity and Oxy plane coincides with the undisturbed free surface. Fig. 1 shows the definition of computation domain. The boundary surfaces for the wavemaker, body, wall and free surface are denoted by S_W, S_B and S_F respectively. Focusing point is denoted by x_b that is the distance from the wavemaker. The diameter of cylinder which is located at focusing point is denoted by D. The length, half width and water depth of the numerical wave tank are defined as L, B and H respectively.

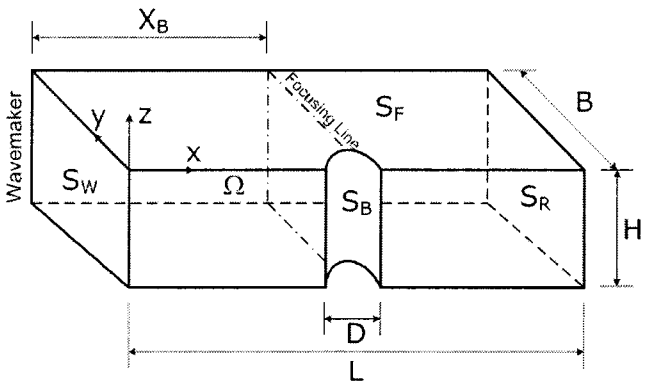

Fig. 1 Definition of computation domain

It is assumed that the fluid is incompressible, inviscid and its motion is irrotational. The surface tension effect is ignored. So there is the velocity potential ϕ which is governed by Laplace equation.

$$\nabla^2\phi = 0 \text{ in } \Omega \tag{1}$$

The nonlinear free surface conditions on $z = \zeta(x,y,t)$ can be given by the following kinematic and dynamic conditions.

$$\zeta_t = \phi_z - \phi_x\zeta_x - \phi_y\zeta_y \text{ on } S_F \tag{2}$$

$$\phi_t = -\frac{1}{2}|\nabla\phi|^2 - g\zeta \text{ on } S_F \tag{3}$$

where g is gravitational acceleration. As an initial condition, it is assumed that the fluid motion is at rest. The wall and body boundary condition is given as follows.

$$\phi = 0 \text{ on } z = -H \tag{4}$$

$$\phi = 0 \text{ on } y = \pm B \tag{5}$$

The boundary condition at the wavemaker is given by following equation.

$$\phi_n = \vec{V} \cdot \vec{n} \tag{6}$$

where $\vec{V}$ is the lateral velocity at the piston-type wavemaker.

3. Time Domain Analysis

Numerical computation on extreme wave produces highly nonlinear free surface elevation such as a sharp crest. For this reason, to analyze the nonlinear free surface problem in time domain, the numerical stability as well as accuracy is very important. In the present study, finite element method based on variational principle is adopted to obtain the stable solution for the given nonlinear free surface problem. By introducing of variation J, the Lagrangian L corresponding to J is obtained as follows.

$$J = \int_0^t L dt \tag{7}$$

$$L = \rho \iint_{S_F} \phi\zeta_t dS - \frac{\rho}{2}\iint_{S_F} g\zeta^2 dS - \frac{\rho}{2}\iiint_{\Omega} |\nabla\phi|^2 dV \tag{8}$$

where ρ is the density of water. Taking the variations on J with respect to ζ and ϕ results in a stationary equation, which is equivalent to the governing equation and free surface conditions as given in Eqs. (1) ~ (3).

To solve the equivalent variational functional given by Eqs. (7) ~ (8), the whole domain is discretized into a number of finite elements. As a basis function for finite element the linear element is adopted. The set of trial function basis is denoted by $\{N_j\}$. Then the potential function ϕ and the surface elevation ζ can be approximated by the span of the bases.

$$\phi = \sum_{j=1}^{M} \phi_j N_j \ , \quad \zeta = \sum_{j=1}^{M_t} \zeta_j N_j \tag{9}$$

where ϕ_j and ζ_j are the node-wise value of velocity potential function and surface elevation in finite element

space, respectively. M is the total number of nodes and M_f is the number of nodes only on free surface. The stationary equation by taking variation of Eq. (8) can be obtained as follows.

$$T_{kj}\dot{\zeta}_j = K_{kj}\phi_j \tag{10}$$

$$T_{kj}\dot{\phi}_j = -\frac{1}{2}\phi_i\frac{\partial K_{kj}}{\partial \zeta_k}\phi_j - gP_{kj}\zeta_j \tag{11}$$

$$K_{ij}\phi_j = 0 \tag{12}$$

where

$$K_{ij} = \iiint_{\Omega} \nabla N_i \cdot \nabla N_j dV \tag{13}$$

$$P_{kj} = \iint_{S_F} N_k N_j dS \tag{14}$$

$$T_{kj} = \iint_{S_F} N_k N_j dS \tag{15}$$

It is well known that the solution of the above discretized problem satisfies the conservation of mass and energy. It is quite interesting to note that Eq. (12), Laplace equation, behaves like constraints for the above two free surface boundary conditions. The more detailed descriptions on the finite element analysis is shown in Kyoung et al.(2005)

4. Frequency Focusing

Frequency-focusing method utilizes the linear wave theory in which the longer wave propagates faster than the shorter wave. Therefore the focused wave can be made in the numerical wave tank as well as the model experiment. The water surface elevation induced by different waves which have similar frequencies can be expressed by the linear wave theory as following way.

$$\eta(x,t) = \sum_{n=1}^{N} a_n \cos(k_n x - 2\pi f_n t - \psi_n) \tag{16}$$

where N is the number of waves and a_n is the wave amplitude corresponding to the wave with frequency f_n. The phase of each wave is denoted by ψ_n. The wave number k_n is given by linear wave theory as follows.

$$(2\pi f_n)^2 = gk_n \tanh k_n H \tag{17}$$

where H is the mean water depth. If x_b is the focusing point and t_b is the focusing time, the phase ψ_n for each wave given in Eq. (16) at focusing point can be rewritten as following equation.

$$\psi_n = 2m\pi + k_n x_b - 2\pi f_n t_b, \; m = 0, \pm 1, \pm 2, \ldots \tag{18}$$

Surface elevation at $x=0$ can be expressed with the phase given in Eq. (18) in following equation when the wavemaker is located at $x=0$.

$$\eta(0,t) = \sum_{n=1}^{N} a_n \cos(-k_n x_b - 2\pi f_n t) \tag{19}$$

Since the focused point is based on the linear wave theory, the focused wave does not generally appear at the given focused point x_b. Therefore it needs some corrections. In the present study, the focusing point $x_b$is obtained by changing t_b since Rapp & Melville(1990) reported that the focusing time t_b given in Eq. (18) does not affect the wave shape at the focusing point.

5. Numerical results

The developed numerical method is validated by comparing with the previous experiment by Chaplin et al. (1997). The length, width and water depth for the numerical validation are taken by 28m, 1.5m and 0.525m, respectively. A bottom-mounted circular cylinder with 0.1m diameter is located at the focusing point which is 12.5m apart from the wavemaker.

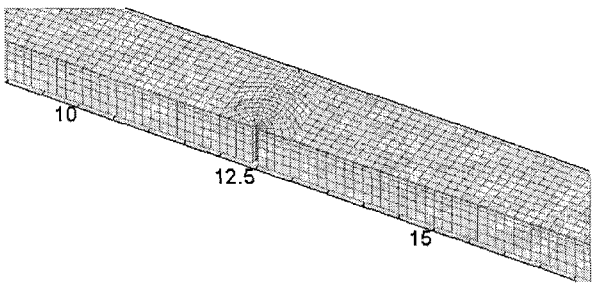

Fig. 2 Grid system using finite elements

The grid space in outer side of the vertical cylinder is taken by 0.1m horizontally while denser grids are applied near the vertical cylinder. The total number of element is taken by 6 vertically.

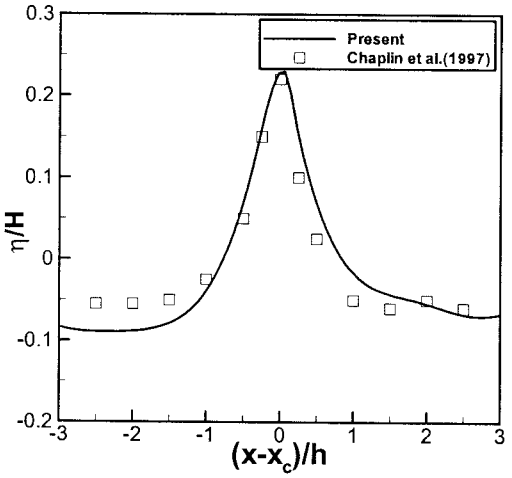

Fig. 3 Spatial distribution of wave elevation around focusing point without vertical cylinder when $A_T K_c = 0.33$

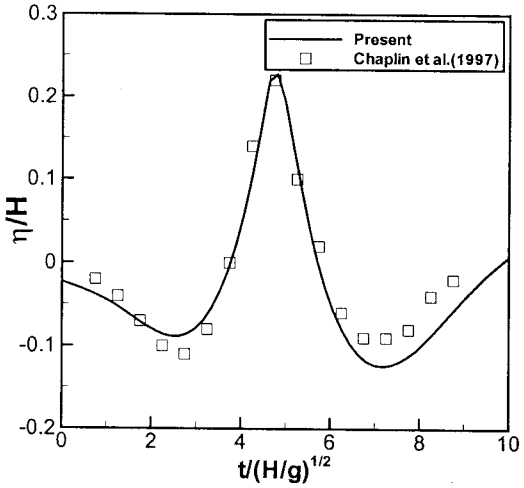

Fig. 4 Time history of wave elevation at focusing point without vertical cylinder when $A_T K_c = 0.33$

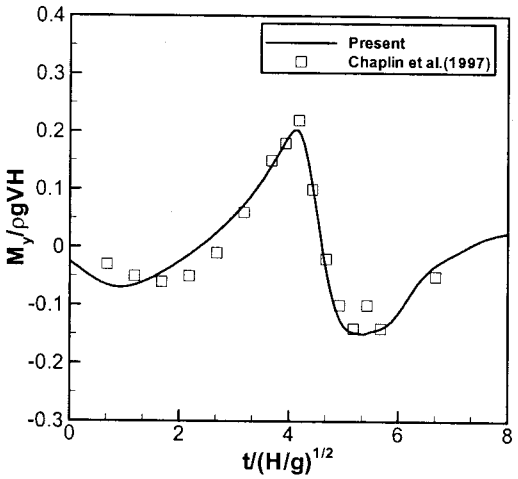

Fig. 5 Time history of bending moment on vertical cylinder when $A_T K_c = 0.33$

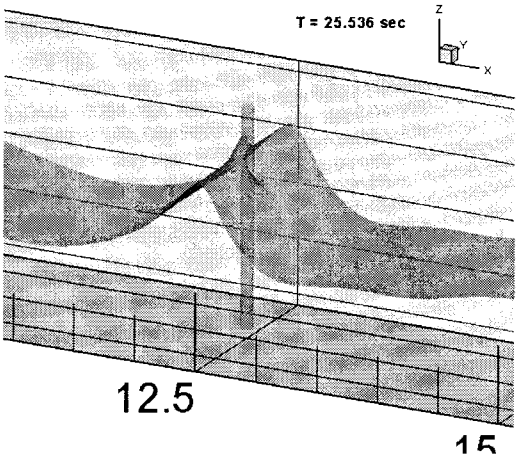

Fig. 6 Wave elevation at the focusing time when $A_T K_c = 0.33$

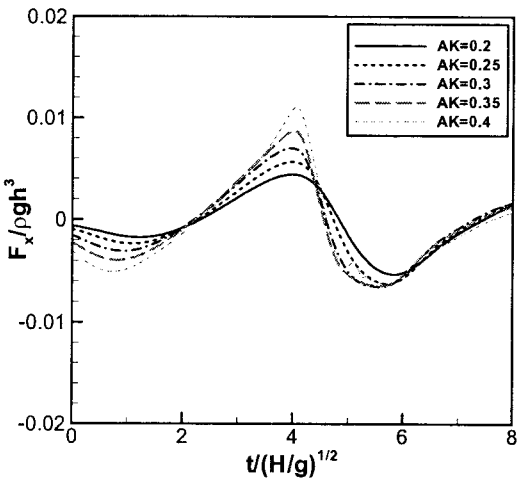

Fig. 7 Time history of wave loads at focusing point by varying wave slope.

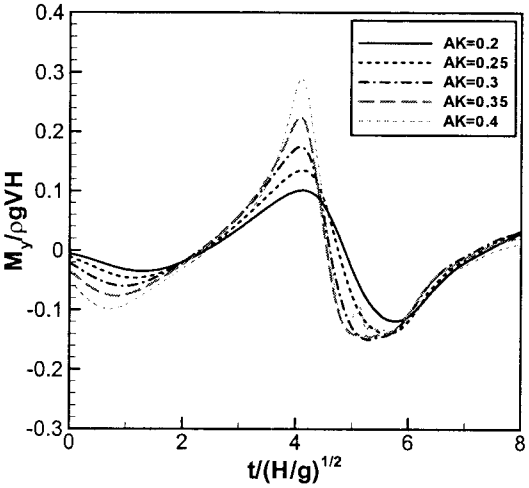

Fig. 8 Time history of bending moments at focusing point by varying wave slope.

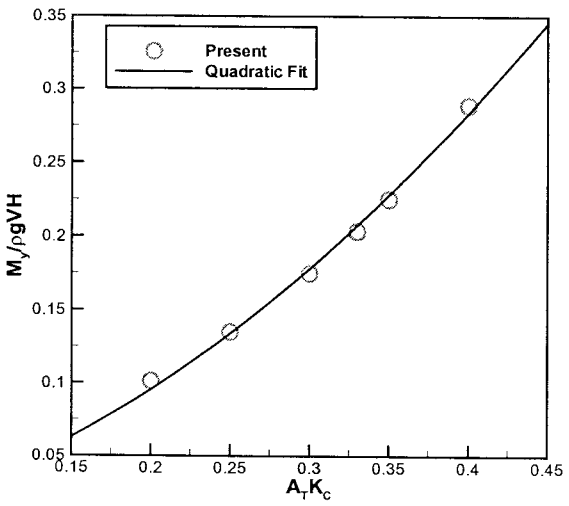

Fig. 9 Maximum bending moments at focusing point by varying wave slope.

Especially the cosine spacing is applied to vertical direction so that the grid spacing becomes denser near the free surface. The typical grid system is shown in Fig. 2.

The wave damping region is located on opposite side to wavemaker to prevent the wave from reflecting. The total number of wave component is taken by 34, which is equally divided($f_1 = 0.511Hz$, $f_{34} = 1.244Hz$). The wave slope is denoted by A_TK_c. A_T is the wave amplitude at focusing point. The wave number K_C is defined by $K_C = K[1/2(f_1 + f_{34})]$. The 4th order Runge-Kutta method is adopted for time integration. The time integration step is taken by $1/(120f_{34})$.

Fig. 3 shows the numerical comparison of spatial distribution of wave elevation without the vertical cylinder when $A_TK_c = 0.33$. The numerical comparison shows a good agreement. Expecially the steep wave profile can be well observed at focusing point.

Time history of wave elevation at the focusing point without vertical cylinder is shown in Fig. 4. The typical extreme wave property that the sharp crest is following by deep trough is well observed. It can be thought that the ocean going vessels or floating offshore structures which encounter the extreme wave have quite a possibility to be capsized.

Fig. 5 shows the time history of bending moment on vertical cylinder. A good agreement can be found when it is compared with the previous study(Chaplin et al., 1997).

Fig. 6 shows the snap shot of wave elevation when the focused wave occurs at the location of the vertical cylinder. Local run-up phenomena on the vertical cylinder can be observed.

Fig. 7 and Fig. 8 show that time history of wave loads and bending moments at the focusing point by varying wave slope. It can be observed that the maximum wave load and bending moment increase as the wave slope increases. In Fig. 9, the maximum of the bending moment shows a quadratic increment as the wave steepness increases in the present numerical computations.

6. Conclusions

In the present study, a numerical method is developed to investigate the wave load induced by the extreme wave. As a numerical method, finite element method based on variational principle is applied. To obtained the focused wave, the frequency focusing of unidirectional wave is utilized. From the comparisons with the previous study, the developed numerical method has a good agreement. In variation of wave slope, it is observed that the wave loads and bending moment tends to become steep as the wave slope increases. Especially it is also noticed that the maximum of the bending moment has a quadratic increment according to the increase of the wave steepness.

Aknowledgements

This present work is a part of both "Development of design technology of VLFS" funded by MOMAF and "Development of Safety Evaluation Technologies for Marine Structures in Disastrous Ocean Waves" supported by Korea Research Council of Public Science & Technology.

References

Chaplin, J.R., Rainey, R.C.T., Yemm, R.W. (1997). "Ringing of a Vertical Cylinder in Waves", Journal of Fluid Mechanics, Vol 350, pp 119-147.

Chaplin, J.R. (1996). "On Frequency-Focusing Unidirectional Waves", International Journal on Offshore and Polar Engineering, Vol 6, No 2, pp 131-137.

Clauss, G. (1999). "Task-Related Wave Groups for Seakeeping Tests or Simulation of Design Storm Waves", Applied Ocean Research, Vol 21, pp 219-234.

Contento, G., Codiglia, R., D'Este, F. (2001). "Nonlinear Effect in 2D Transient Nonbreaking Waves in a Closed Flume", Applied Ocean Research, Vol. 23, pp. 3-13.

Grue, J. (2002). "On Four Highly Nonlinear Phenomena in Wave

Theory and Marine Hydrodynamics", Applied Ocean Research, Vol 24, pp 261-274.

Hong, K.Y., Liu, S.X., Hong, S.W. (2002). "Theoretical Study on the Generation of Directional Extreme Waves", Journal of the Society of Naval Architects of Korea, Vol 39, No 1, pp 38-48.

Kim, J.W., Kyoung, J.H., Bai, K.J., Ertekin, R.C. (2004). "A Numerical Study of Nonlinear Diffraction Force on Floating Bodies due to Extreme Transient Waves", 25th Symposium on Naval Hydrodynamics, pp 105-115.

Kyoung, J.H., Hong, S.Y., Kim, J.W. and Bai, K.J. (2005). "Finite-element computation of wave impact load due to a violent sloshing", Ocean Engineering, Vol 32, pp 2020-2039.

McLean, J.W. (1982). "Instabilities of Finite-Amplitude Water Waves", J. Fluid Mech., Vol 114, pp 315-330.

Osborne, A.R. (2001). "The Random and Deterministic Dynamics of Rogue Waves in Unidirectional, Deep Water Wave Trains", Marine structures, Vol 14, No 3, pp 275-293.

Peregrine, D.H. (1976). "Interaction of Water Waves and Currents", Advanced Applied Mechanics, Vol 16, pp 9-117.

Rapp, R.J., Melville, W.K. (1990). "Laboratory Measurements of Deep-Water Breaking Waves", Phil. Trans. R. Soc. Lond. A 331, pp 735-800.

Smith, S., Swan C. (2002). "Extreme Two-Dimensional Water Waves: An Assessment of Potential Design Solutions", Ocean Engineering, Vol 29, pp 387-416.

Trulsen, K and Dysthe, K.B. (1997). "Freak Waves: A 3-D Wave Simulation", Proc. 21st Int. Symp. on Naval Hydrodyn., Trondheim, Norway.

Zou, J., Kim, C. (1995). "Extreme Wave Kinematics and Impact Loads on a Fixed Truncated Circular Cylinder," Proc. 5th Int. Offshore and Polar Eng. Conf., pp 216-225.

2000년 0월 0일 원고 접수
2000년 0월 0일 최종 수정본 채택